[CANCER RESEARCH 63, 4331–4337, August 1, 2003]

Advances in Brief

Expulsion of Small Molecules in Vesicles Shed by Cancer Cells: Association with Gene Expression and Chemosensitivity Profiles[1,2]

Kerby Shedden, Xue Tao Xie, Parthapratim Chandaroy, Young Tae Chang, and Gustavo R. Rosania[3]

Department of Statistics, University of Michigan, Ann Arbor, Michigan 48109 [K. S.]; Department of Pharmaceutics, University of Michigan College of Pharmacy, Ann Arbor, Michigan 48109 [X. T. X., P. C., G. R. R.]; and Department of Chemistry, New York University, New York, New York [Y. T. C.]

Abstract

Anticancer drug resistance results from selective pressure of chemotherapy, together with mutations or epigenetic changes that make cells refractory to treatment. In cancer cells, we report that gene expression associated with vesicle shedding correlates with chemosensitivity profiles. Experiments with doxorubicin and other small molecules confirm drug accumulation and expulsion in shed vesicles. Relative differences in the rate of vesicle shedding correspond with doxorubicin resistance across various cell lines. Moreover, accumulation of drug in membrane domains in which vesicles originate accounts for drug expulsion in shed vesicles. These observations implicate vesicle shedding as a drug efflux mechanism potentially involved in drug resistance.

Introduction

In many noncancerous cells, vesicle shedding is considered to be physiologically important. During erythrocyte differentiation, for example, membrane proteins and lipid components destined for removal from the erythrocyte membrane are eliminated via shed vesicles, sometimes referred to as exosomes (1–3). Dendritic cells of the immune system also shed exosomes (4–7). When released into the blood stream, exosomes can present antigen to T-lymphocytes located at distant sites. Cancer cells have been found to shed large numbers of vesicles or exosomes, both *in vitro* and *in vivo* (6, 8–11). Vesicles shed by cancer cells are highly immunogenic (5, 9, 11–13) and harbor metalloproteases potentially associated with metastasis (8, 14–16). Nevertheless, despite their presence in many cancer cell types that have been analyzed, the significance of vesicle shedding in cancer cell biology is an open question.

Materials and Methods

Cell Culture, Microscopy, and Flow Cytometry. All of the cell lines were obtained from the Developmental Therapeutics Program at NCI.[4] Cells were maintained in 5% CO_2 at 37°C in RPMI 1640 supplemented with 10% fetal bovine serum and penicillin-streptomycin. Cell culture medium was centrifuged at 100,000 × *g* for 1 h, followed by filtering through a 0.2 μM filter, to get rid of extraneous vesicles and particles. Cells were plated on Greiner glass-bottomed 96-well plates at least 24 h before the experiments. Styryl library was screened as described previously, on UACC-62 cells (17). For doxorubicin pulse-chase experiments using time-lapse microscopy and flow cytometry, MCF7 cells were pulsed with drug for 1 h at 4 μM concentration, after which any free vesicles were removed from the cells by vigorous flushing with a hand-held electronic pipetor. To assay the effect of the treatment of cell viability, cell growth was assayed 48 h later with the MTS reagent (Promega). For flow cytometric analysis, MCF-7 cells were washed and flushed with a handheld pipetor to remove released vesicles. The medium with the vesicles was centrifuged for 5 min at 13,000 rpm on a table-top microcentrifuge (to remove any contaminating cells), and the vesicles were then analyzed with a FACScalibur flow cytometer (Becton Dickinson).

Shed Vesicle Isolation and Fractionation. For biochemical analysis of shed vesicles, cells were grown to 50% confluency. At that time, the medium was replaced, and the cells were allowed to grow to confluency for 48 h; the conditioned medium was then collected. Shed vesicles, loosely bound to the surface of the cells, were then released using a mild trypsin digestion in calcium-free medium, followed by vigorous flushing. Released vesicles were pooled and spun down at 1000 × *g* for 10 min to remove any floating cell and debris. Cell-free supernatant was then transferred to ultracentrifuge tubes and spun down at 100,000 × *g* for 1 h. To remove free drug, the resulting vesicle pellet was suspended in excess HBSS buffer and spun down again. The identity of these vesicles could be established based on staining with doxorubicin or styryl molecules that specifically stained cell-surface vesicles. For further fractionation, the suspended vesicle pellet could be overlayed on a 30–40% Percoll gradient and spun for 2 h at 100,000 × *g*. To characterize the size of the vesicles present in the medium, dynamic light-scattering analysis was performed using a particle sizer (NICOMP Instruments, Santa Barbara, CA). To compare the rates of vesicle shedding in different cell lines, isolated vesicles were incubated with 0.1% Triton X-100, after which protein content was measured using a BCA assay (Pierce) with BSA dilutions as standards.

Doxorubicin Binding. Doxorubicin solutions were made from a 3-mM stock in double-distilled H_2O and were centrifuged through an Amicon ultrafiltration membrane (cutoff M_r <100,000) to remove any aggregates or particles. Isolated vesicles were incubated with doxorubicin overnight at 37°C. After incubation, doxorubicin fluorescence associated with the vesicles was analyzed either microscopically using an epifluorescence microscope equipped with a digital camera or biochemically using a homogeneous fluorescence assay of doxorubicin content.

Microscopic Analysis of Doxorubicin Binding to Individual Vesicles. Microscopic images of the doxorubicin-containing vesicles on glass coverslips were acquired using a 100X Zeiss Oil Immersion objective, with doxorubicin-specific filter set (excitation, 490 nm; dichroic, >510 nm; emission, >570 nm). Doxorubicin fluorescence in individual vesicles was measured using image analysis software (Metamorph; Universal Imaging, Inc.). For each measured vesicle, the outline of the particle was traced manually, and the integrated fluorescence intensity over the entire area of each vesicle was graphed against the calculated vesicle volume ($V = 4/3\ \pi\ r^3$, where r is the radius of the vesicle). For each doxorubicin concentration, at least 10 vesicles were measured and graphed. The slope of the resulting linear fit of each graph (intercept = 0,0) was used as a measure of doxorubicin accumulation (units, doxorubicin fluorescence/vesicle volume) at that concentration. To incorporate result sets obtained from experiments performed on different days, we normalized each set of doxorubicin accumulation values by dividing with the maximum value of the corresponding set.

Homogeneous Fluorescence Assay of Doxorubicin Content. Doxorubicin-containing vesicles were ultracentrifuged at 100,000 × *g* for 1 h, and the vesicle pellet was washed in HBSS. The suspended pellet was placed in a Microcon ultrafiltration device (M_r cutoff, 100,000). The device was spun to dryness at 13,000 rpm in a bench-top microcentrifuge. For measurement,

Received 3/10/03; accepted 6/18/03.

The costs of publication of this article were defrayed in part by the payment of page charges. This article must therefore be hereby marked *advertisement* in accordance with 18 U.S.C. Section 1734 solely to indicate this fact.

[1] Supported by the University of Michigan Bioinformatics Program, Pfizer Inc. Central Research (Ann Arbor), and Howard Hughes Medical Institute (to K. S. and G. R. R.).

[2] Supplementary data for this article are available at *Cancer Research Online (http://cancerres.aacrjournals.org).*

[3] To whom requests for reprints should be addressed, at University of Michigan College of Pharmacy, 428 Church Street, Ann Arbor, MI 48109. E-mail: grosania@umich.edu.

[4] The abbreviations used are: NCI, National Cancer Institute; 5-FU, 5-fluorouracil; HPLC, high-performance liquid chromatography; ECM, extracellular matrix; CDK, cyclin-dependent kinase; PI, propidium iodide; TCNP, triciribine phosphate.

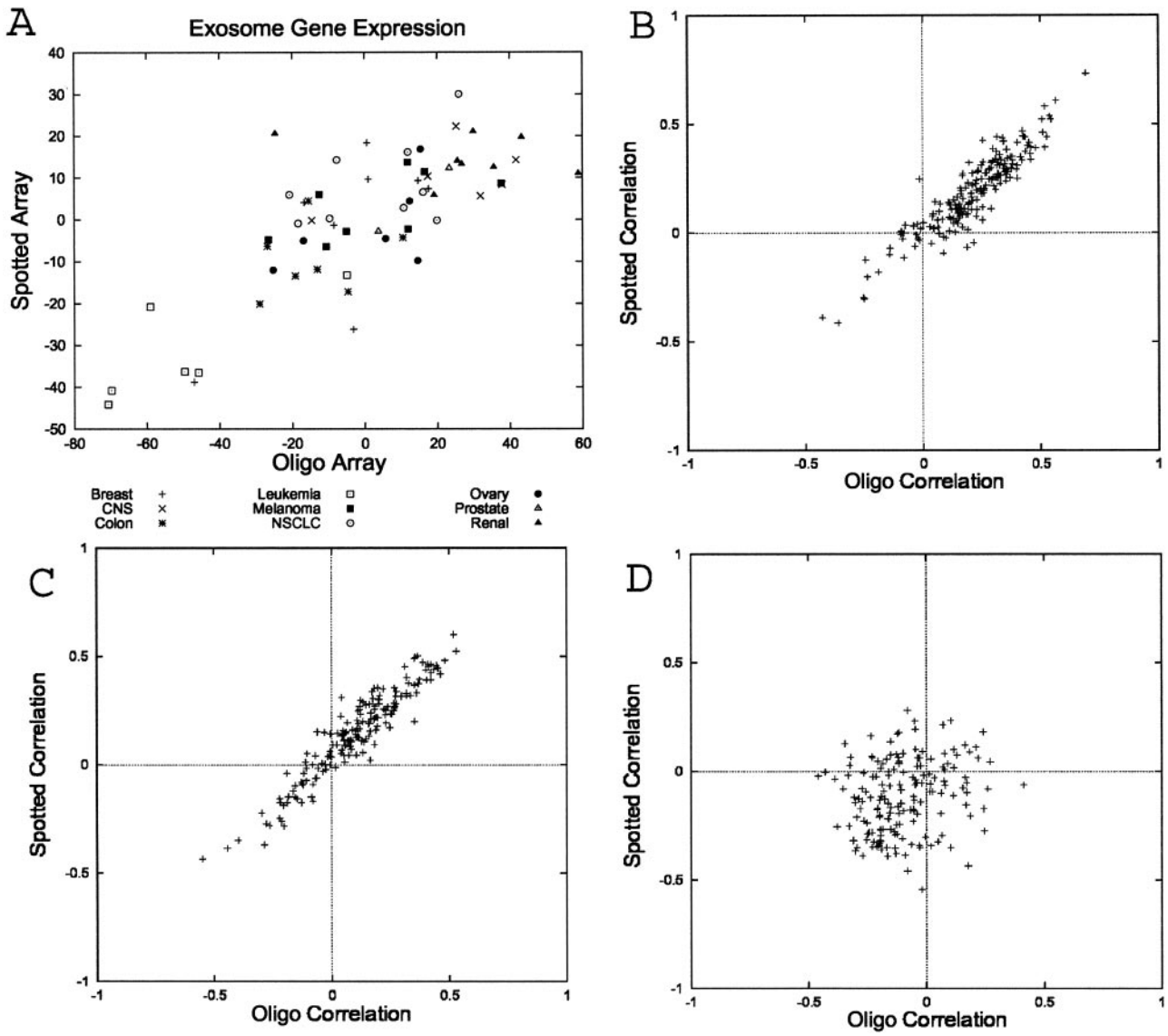

Fig. 1. Analysis of gene expression data. *Ordinate* represents the relative expression of the vesicle-shedding index as obtained from the spotted array (19), and *abscissa* shows the corresponding oligonucleotide array data (18). *A*, comparative analysis of the normalized vesicle-shedding index, for each one of the cell lines in the NCI 60-cell-line panel. *Each data point* represents a different cell line. *B–D*, plots of the correlation between different gene expression indices and GI_{50}, for each of the 171 drugs of the standard anticancer agent database (*B*, vesicle-shedding index; *C*, ECM index; *D*, cell cycle index).

trapped doxorubicin in the vesicles was completely released from the filter by adding 1–10% SDS and spinning again. For analysis, doxorubicin-containing detergent extract was transferred to 96-well plates, and the fluorescence was read with a Typhoon fluorescence scanner (excitation, 490; emission, >560 nm; Amersham Biosciences). Actual doxorubicin content is calculated based on doxorubicin standards of known concentration.

HPLC Analysis of Drug Binding. To detect the association of the four different molecules (staurosporine, PI, TCNP, and 5-FU) with shed vesicles, the shed vesicles were incubated with equivalent concentration (20 μM) of one of the four different molecules along with 20 μM doxorubicin, overnight at 37°C and presence of the associated molecules was measured using HPLC after isolating the shed vesicles, as described in the previous section. The HPLC absorbance was converted into concentration based on peak areas obtained with standards of known concentration. The results are based on triplicate sample measurements. In all of the samples analyzed, doxorubicin was readily detectable by fluorescence and served as the internal control. In several samples, the concentration of the other molecule analyzed was not detected. In all cases, the lowest measurable drug concentration was less than 5% of the doxorubicin concentration, confirming that the drug was largely absent from samples.

Microarray and Chemoinformatic Data Sources and Preprocessing. Bioinformatic analysis was based on microarray measurements of gene expression and of chemosensitivity that have been previously published and made publicly available (18, 19). The measurements were made on a reference set of 60 cell lines (known as the NCI 60 cell lines) covering nine tumor types. Two-channel (spotted) microarray measurements (19) were obtained from http://genome-www.stanford.edu/sutech/download/nci60/index.html. Single-channel (oligonucleotide) microarray measurements (18) were obtained from http://www.genome.wi.mit.edu/MPR/NC160/NC160.html. The single-channel data were scaled so that each array had a mean expression of 1500 units; then the transform $\log_2[50 + \max(X + 50; 0)]$ was applied. The two-channel microarray data were measured as described previously (19) to produce $\log_2$ transformed values. We eliminated transcripts that were missing on more than four arrays and imputed the remaining missing values using the mean of the observed values (on the log scale) for the same transcript. Measurements of GI_{50} (the concentration of drug at which cell growth is inhibited by 50%) were obtained for 171 drugs from the NCI "Standard Anticancer Agent Database",[5]

[5] Internet address: http://dtp.nci.nih.gov/docs/cancer/searches/standard_agent_table.html.

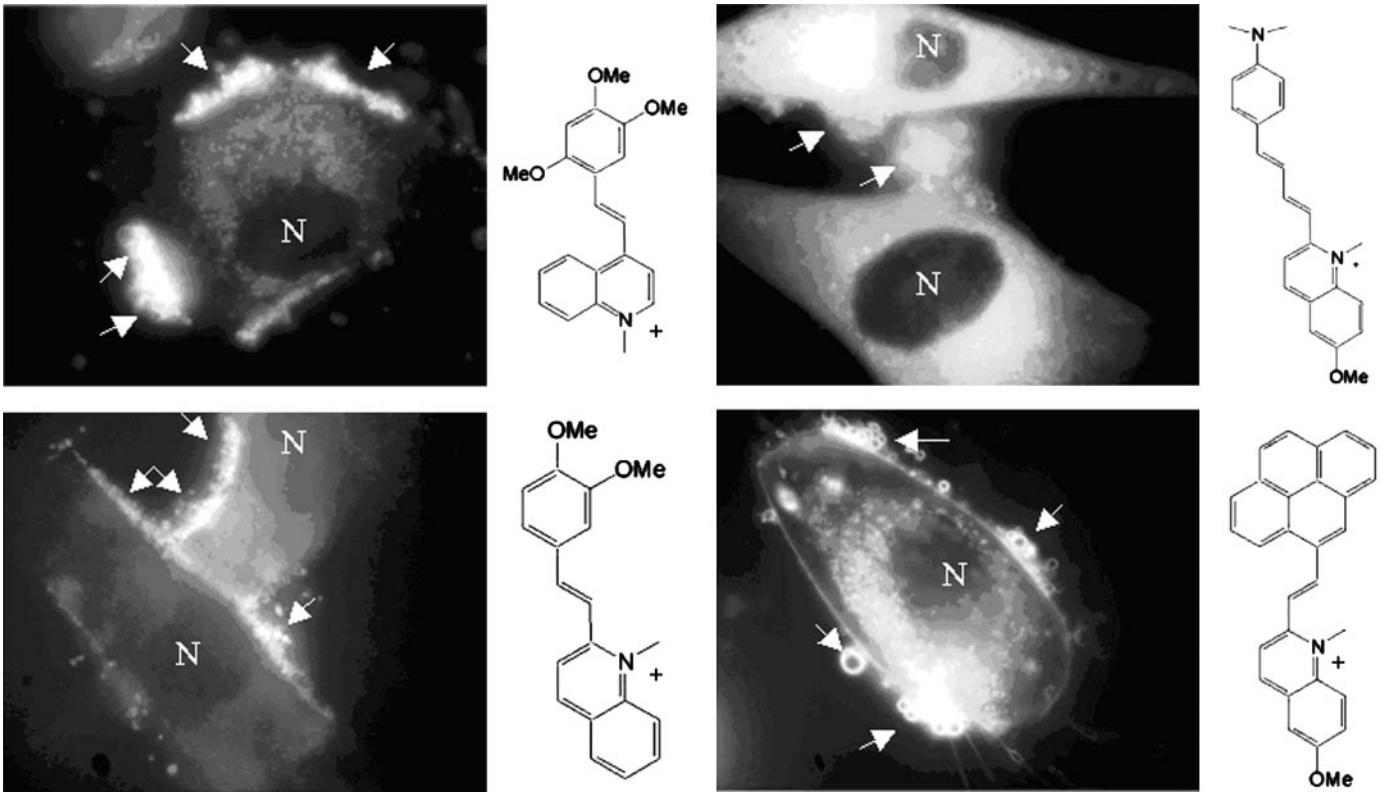

Fig. 2. Fluorescent styryl dyes accumulate in vesicles on the surface of cancer cells. *Arrows*, vesicles labeled with the styryl compound shown at the right of each image. These vesicles appear to be loosely associated with the cell margins. Note that different lipophilic styryl compounds exhibit different intracellular staining patterns, but they all appear present in association with shed vesicles. *Bar*, 10 μm.

a collection of chemical agents with well-understood mechanisms of action and clinical relevance. The GI_{50} values were $\log_2$ transformed, and missing values were imputed with the mean overall cell lines for a given drug.

Identification of Relevant Gene Sets. For creating a vesicle shedding (or "exosome") index, genes identified in the literature (reviewed in Ref. 4) were matched to genes in the microarray or oligonucleotide platforms based on their names. For example, if actin was found in exosomes, all of the gene names containing "actin" were included in the vesicle-shedding (or exosome) index. For comparisons, we selected ribosomal genes, immunoglobulins, ECM components, genes coding for serum proteins, transporters, and cell-cycle control genes including cyclins, CDK, and CDK inhibitors. These terms were then matched to specific genes on either of the two microarray platforms. The actual values for the index were constructed by totaling the mean centered expression levels for those genes in the lists.

Statistical Analysis of Gene Expression and Chemosensitivity Profiles. We assessed the association of gene expression with chemosensitivity using correlation coefficients. The Pearson correlation coefficient was used to measure the relationship between gene expression and GI_{50}. We also computed the proportion of genes that have specifically low or high expression in one of the nine tumor classes. That is, a gene counts toward the proportion if the expression is more than 2-fold higher in one class than in any of the other classes, or more than 2-fold lower in one class than in any of the other classes.

Results and Discussion

Analysis of Gene Expression and Chemosensitivity Profiles. As a hypothesis, we considered the possibility that anticancer drug resistance and vesicle shedding could be mechanistically related, based on drug expulsion in association with shed vesicles. Because of the small size of shed vesicles, steady-state turnover of specific vesicle-associated proteins should be high; however, nonspecific turnover of trapped cytoplasmic components should be low, given the high surface-to-volume ratio of the vesicles. If vesicle shedding serves as a mechanism for drug expulsion, we hypothesized that overexpression of genes associated with shed vesicles would correlate with anticancer drug resistance.

To test this hypothesis, chemosensitivity profiles of the standard anticancer agent database of the Developmental Therapeutics Program (DTP) at the NCI was analyzed relative to the gene expression profiles of the NCI 60-cell-line panel (18, 19). To quantify membrane shedding-related gene expression, an "index" was constructed, composed of genes previously found to be present in shed vesicles or exosomes, based on previous proteomic analysis or immunoblotting experiments (reviewed in Ref. 4). This vesicle-shedding index was found to be consistent in two different transcriptional profiling experiments performed on the NCI panel of 60 cancer cell lines, one using oligonucleotide arrays and the other using spotted arrays (Fig. 1*A*). This suggests that a reproducible biological process, nominally related to membrane shedding, is tracked by the index. A notable feature of the vesicle-shedding index across the 60-cell-line panel is that there is a strong relationship between the index and tissue type; vesicle-shedding-related gene expression is strongest in solid tumor and weakest in leukemic cell lines.

Looking at correlations between the shedding index and GI_{50} for each of the 171 compounds in the NCI standard anticancer agent database reveals a predominance of positive relationships (Fig. 1*B*). This supports the hypothesis that vesicle shedding and drug resistance are related. Although the relationship is weak for many of the drugs, the trend is reproducible across the two platforms. Moreover, across a large number of drugs having diverse mechanisms of action, the shedding index is positively associated with GI_{50} 87% of the time. The correlation of doxorubicin GI_{50} with the shedding index is 0.37. Although modest in magnitude, this correlation is statistically significant at the 0.01 level. Notably, more

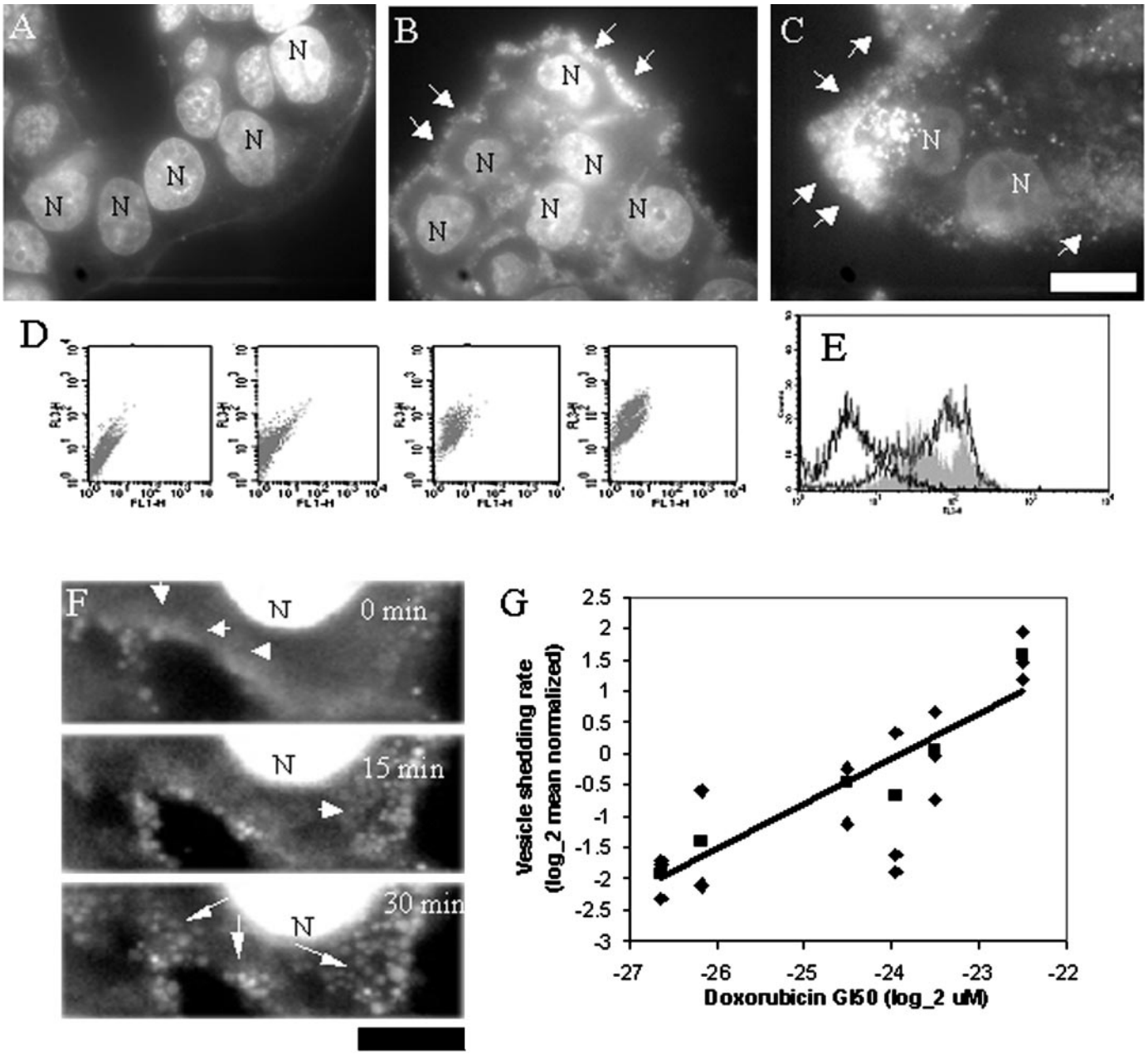

Fig. 3. *A–F*, pulse-chase experiments with doxorubicin and MCF7 cells. *A*, immediately after the pulse and chase, doxorubicin fluorescence is localized to the nucleus (*N*). *B*, 3 h later, doxorubicin fluorescence is in vesicles at the cell margins (*arrows*). *C*, 24 h later, doxorubicin fluorescence is found mostly associated with shed vesicles (*arrows*). *Bar*, 10 μm. *D*, flow cytometric analysis of conditioned media, after pulse-chase experiment with doxorubicin. Plots show FL3 channel fluorescence in ordinate (doxorubicin) against FL1 channel fluorescence in abscissa (background autofluorescence). *From left to right*, 0, 1.25, 4, and 10 μM doxorubicin pulse. *E*, time course assay of doxorubicin fluorescence in vesicles shed by MCF7 cells. Plots correspond to vesicle fluorescence from untreated cells (*left most peak*) and from vesicles harvested 2 h (*filled gray curve*) and 24 h (*right most peak*) after doxorubicin pulse. *F*, time-lapse analysis of doxorubicin accumulation in vesicles. Doxorubicin first accumulates in distinct domains at the cell margin (*arrowheads*) that fragment into distinct vesicles (*arrows*); *N*, the nuclei; *bar*, 5 μm. *G*, relationship between the rate of vesicle shedding and doxorubicin GI_{50} for six different cell lines (in order of increasing GI_{50}): MOLT4, MCF7, K562, ACHN, RPMI8226, CAKI1. Average vesicle-shedding rate (■) was determined, based on three independent measurements performed on three different days (◆).

than 50 of the 171 drugs in the standard anticancer agent database surpass doxorubicin in terms of the calculated correlation.

For comparison, we constructed expression indices from genes associated with other biological processes. Among all of these, correlations for the ECM index were predominantly positive, but less so than that for the vesicle-shedding index (Fig. 1*C*). The ECM-GI_{50} correlation can be explained as a consequence of the differences in drug resistance between the leukemic *versus* solid tumor progenitor cells (leukemic cells do not have an ECM). Another control shows the correlation between GI_{50} and a cell cycle expression index that tracks average expression of cyclins and CDKs minus the average expression of CDK inhibitors (Fig. 1*D*). In this case, the correlations are small, nonreproducible between the two platforms, and lack any tendency to be positive or negative.

Seeking a deeper understanding of how the vesicle-shedding index is influenced by the individual genes that comprise it, each gene in the index was analyzed for evidence of tumor-specific expression. Supplementary Tables 1 and 2^2 list the genes on the two microarray platforms that comprise the vesicle-shedding index, along with the tissues in which each gene is repressed or overexpressed. Of 108 genes on the oligonucleotide array, 13 genes are repressed in leukemia cell lines. Moreover, these 13 genes all fall in the top one-third of the

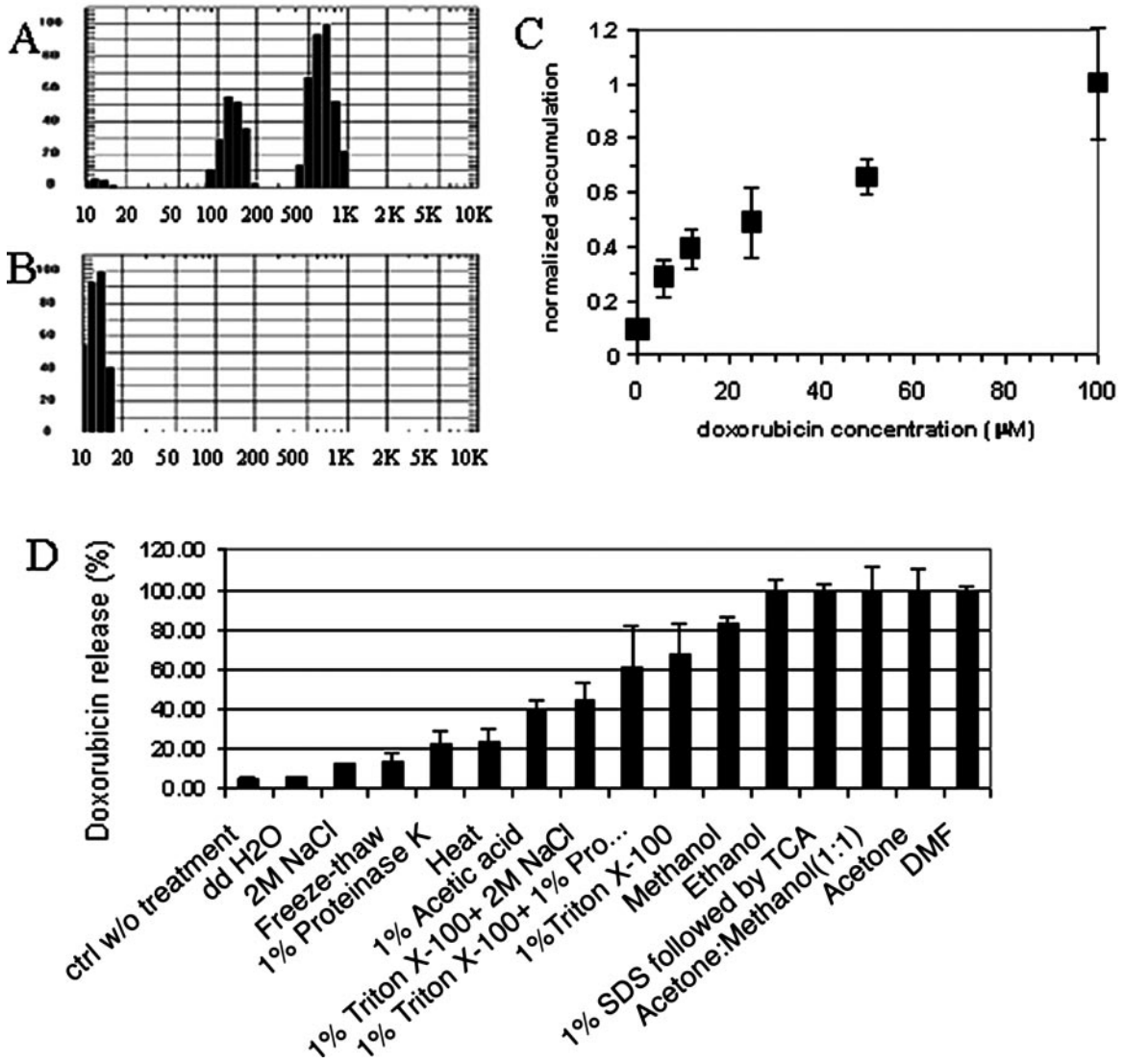

Fig. 4. *A*, size distribution of particles in MCF7-conditioned media, determined by dynamic light scattering. *B*, size distribution of particles in cell-free media. *C*, plot of doxorubicin accumulation in isolated vesicles as a function of added doxorubicin concentration. *D*, doxorubicin extraction from isolated shed vesicles in the presence of a variety of treatments. *Ctrl w/o treatment*, control; *TCA*, trichloroacetic acid; *DMF*, dimethylformamide.

list in terms of total abundance. The presence of 13 of 108 genes that are repressed in leukemia cell lines among the genes in the index is far in excess of the 2.2% of genes overall that are repressed in leukemia cell lines. This suggests that genes implicated in vesicle shedding in solid tumor cells may be selectively up-regulated relative to leukemic cells.

Validating the Role of Vesicle Shedding in Drug Expulsion. In parallel with the bioinformatic analysis of gene expression and chemosensitivity data, a library of fluorescent styryl compounds (17) was screened for sequestration and elimination in subcellular compartments in cancer cells. With some of these compounds, a gradual accumulation of fluorescent molecules in vesicles present on the surface of cells became evident (Fig. 2). Together with the bioinformatic analysis described above, these results led us to further consider the role of vesicle shedding as a potential mechanism of drug expulsion.

Pulse-chase experiments with doxorubicin, a fluorescent anticancer drug, confirmed the hypothesis that anticancer drug expulsion can occur via shed vesicles (Fig. 3). Immediately after the drug was pulse-chased, doxorubicin localized to the nucleus (Fig. 3*A*). Three h later, the drug was also present in cytoplasm and in vesicles at the cell margins (Fig. 3*B*). Twenty-four h later, nuclear fluorescence was significantly decreased, and most of the visible doxorubicin was present in extracellular vesicles loosely associated with the cell periphery (Fig. 3*C*). We established that this short pulse with 4 μM doxorubicin had no significant effect on cell viability, as determined 24 and 48 h later with the MTS assay (data not shown) and by the lack of nuclear fragmentation normally seen in dying cells. This experiment indicated that vesicles shed by cancer cells are able to carry the drug.

Encapsulation and expulsion of doxorubicin in vesicles shed into the surrounding medium was confirmed by flow cytometric analysis of cell culture medium conditioned by cancer cells. In dose-response assays (Fig. 3*D*), doxorubicin fluorescence in shed vesicles appeared proportional to the dose, at the concentrations tested. In time course assays, an increase of vesicle-associated doxorubicin fluorescence could be observed between 2 h and 24 h after the pulse (Fig. 3*E*), consistent with microscopic observations. For these experiments, synthetic, 200-nm diameter liposomes, loaded with different concentrations of doxorubicin, were used as positive controls to monitor doxorubicin-specific fluorescence (data not shown).

The formation of doxorubicin-containing vesicles could be di-

rectly monitored in living cells by time-lapse video microscopy (Fig. 3*F*). In pulse-chase experiments, formation of doxorubicin-vesicles occurred in three stages: from a diffuse fluorescence pattern, drug fluorescence accumulated in patches, which eventually fragmented into distinct vesicle-like structures (Fig. 3*F*). A simple calculation suggested that doxorubicin accumulates in the vesicles, above its cytoplasmic concentration; at the concentration of added doxorubicin (4 μM), one would expect, on average, <10 molecules of doxorubicin (based on the volume of the smallest, 200-nm diameter particles). Unless the drug was concentrated in the vesicles, they would have been undetectable given the high background cytoplasmic fluorescence.

Consistent with trends in gene expression data, relative differences in the rates of vesicle shedding in several cancer cell lines analyzed corresponded with trends in doxorubicin resistance. Six different cancer cell lines were analyzed in terms of their relative rates of vesicle shedding per cell. Relative rates of vesicle shedding were compared with doxorubicin GI_{50} concentrations (Fig. 3*G*). The measured correlation between the relative rates of vesicle shedding and the established doxorubicin growth-inhibitory activity is statistically significant ($P < 0.05$), lending further support to the notion that these two phenomena are mechanistically related.

Mechanism of Doxorubicin Accumulation in Shed Vesicles. In the absence of added drug or other exogenous fluorescent tracers, dynamic light scattering measurements of cell-conditioned media confirmed the presence of vesicles shed by cancer cells, indicating that vesicle shedding was a constitutive process. Two distinct populations of shed particles were present in MCF7-conditioned media (100–200 nm and 400-1000 nm; Fig. 4*A*). In contrast, cell culture media alone contained only particles <20 nm in diameter (Fig. 4*B*). Similar experiments confirmed the presence of shed vesicles in conditioned media of several other tumor cell lines [PC3 (prostate), KM12 (colon), UACC-62 (melanoma); data not shown]. Shed vesicles of 400-1000-nm diameters could be isolated from conditioned medium by ultracentrifugation. Confirming their identity, styryl compounds that specifically stained the surface of cells also stained isolated vesicles (data not shown).

Shed vesicles isolated from MCF7-conditioned media were found to passively accumulate and retain doxorubicin, suggesting that simple thermodynamic binding interactions may explain the accumulation of drug in shed vesicles. Incubating isolated vesicle preparations with different doxorubicin concentrations allows the monitoring of passive affinity for drug with shed vesicles (Fig. 4*C*). To explore the mechanism of doxorubicin sequestration in shed vesicles, we probed the nature of the binding interaction biochemically (Fig. 4*D*). Doxorubicin could not be released from vesicles by incubation with hypotonic media (double-distilled H_2O), suggesting that the drug is sequestered in an osmotically insensitive compartment. Treatment with high salt (2 M NaCl) and with proteinase K released less than 20% of drug. Nevertheless, 80–100% of bound drug was released by treatment with methanol, ethanol, acetone, dimethyl formamide, or 1% SDS. Treatment with low concentrations of nonionic detergent followed by proteinase K or high salt did not lead to a significantly greater amount of doxorubicin release relative to detergent treatment alone. Thus, the interaction of doxorubicin and shed vesicles appears to be exclusively sensitive to extraction conditions that disrupt hydrophobic interactions, suggesting the formation of complexes with lipid.

As controls, we tested the association of different molecules with shed vesicles. TCNP, 5-FU, and staurosporine were selected because they are molecules in the standard anticancer agent database that are least correlated with vesicle shedding-associated gene expression (5-FU-GI_{50}:microarray correlation = 0.11; TCNP-GI_{50}:microarray correlation = 0.03; staurosporine-GI_{50}:microarray correlation = -0.38). PI was selected because it is a well-known membrane-impermeant dye. In all cases, the measured affinity of molecules was considerably lower than the affinity of doxorubicin for shed vesicles (doxorubicin, 100%, internal control; staurosporine, 6.7 ± 7.5%; PI, 3.3 ± 1.5%; TCNP, $<0.78\%$; 5-FU, $<5.6\%$). PI and TCNP are charged and hydrophilic; therefore, it is not surprising that they show the least association with shed vesicles. Nevertheless, both 5-FU and staurosporine are cell permeable; yet they show little affinity for shed vesicles. This indicates that lipophilicity or membrane permeability are not the only determinants of doxorubicin's affinity for shed vesicles.

In conclusion, correlation between vesicle-shedding-associated gene expression and anticancer drug resistance trends across the NCI 60-cell-line panel prompt further exploration of the physiological relevance of vesicle shedding in relation to the mechanism of drug expulsion. The associations between shedding-related gene expression, measured rates of vesicle shedding, and chemosensitivity, together with the observation that doxorubicin associates with shed vesicles, indicate that vesicle shedding can serve as a mechanism of drug expulsion. Although plasma membrane transporters like P-glycoprotein are an important mechanism of efflux for drugs in the aqueous phase (20), lipophilic drugs with high affinity for nucleic acids, cellular macromolecules, lipid membranes, or organelles are likely to be present at low concentrations in the aqueous phase of the cytosol. We propose that by virtue of their hydrophobic character, these molecules may be good substrates for shuttling to the plasma membrane via vesicle-mediated traffic, for final elimination in complex with shed vesicles.

References

1. Johnstone, R. M., Mathew, A., Mason, A. B., and Teng, K. Exosome formation during maturation of mammalian and avian reticulocytes: evidence that exosome release is a major route for externalization of obsolete membrane proteins. J. Cell Physiol., *147:* 27–36, 1991.
2. Johnstone, R. M., and Ahn, J. A common mechanism may be involved in the selective loss of plasma membrane functions during reticulocyte maturation. Biomed. Biochim. Acta, *49:* S70–75, 1990.
3. Johnstone, R. M., Adam, M., Hammond, J. R., Orr, L., and Turbide, C. Vesicle formation during reticulocyte maturation. Association of plasma membrane activities with released vesicles (exosomes). J. Biol. Chem., *262:* 9412–9420, 1987.
4. Thery, C., Zitvogel, L., and Amigorena, S. Exosomes: composition, biogenesis and function. Nat. Rev. Immunol., *2:* 569–579, 2002.
5. Zitvogel, L., Fernandez, N., Lozier, A., Wolfers, J., Regnault, A., Raposo, G., and Amigorena, S. Dendritic cells or their exosomes are effective biotherapies of cancer. Eur. J. Cancer, *35* (Suppl. 3)*:* S36–S38, 1999.
6. Denzer, K., Kleijmeer, M. J., Heijnen, H. F., Stoorvogel, W., and Geuze, H. J. Exosome: from internal vesicle of the multivesicular body to intercellular signaling device. J. Cell Sci., *113:* 3365–3374, 2000.
7. Clayton, A., Court, J., Navabi, H., Adams, M., Mason, M. D., Hobot, J. A., Newman, G. R., and Jasani, B. Analysis of antigen presenting cell derived exosomes, based on immuno-magnetic isolation and flow cytometry. J. Immunol. Methods, *247:* 163–174, 2001.
8. Ginestra, A., Miceli, D., Dolo, V., Romano, F. M., and Vittorelli, M. L. Membrane vesicles in ovarian cancer fluids: a new potential marker. Anticancer Res., *19:* 3439–3445, 1999.
9. Wolfers, J., Lozier, A., Raposo, G., Regnault, A., Thery, C., Masurier, C., Flament, C., Pouzieux, S., Faure, F., Tursz, T., Angevin, E., Amigorena, S., and Zitvogel, L. Tumor-derived exosomes are a source of shared tumor rejection antigens for CTL cross-priming. Nat. Med., *7:* 297–303, 2001.
10. Carr, J. M., Dvorak, A. M., and Dvorak, H. F. Circulating membrane vesicles in leukemic blood. Cancer Res., *45:* 5944–5951, 1985.
11. Andre, F., Schartz, N. E., Movassagh, M., Flament, C., Pautier, P., Morice, P., Pomel, C., Lhomme, C., Escudier, B., Le Chevalier, T., Tursz, T., Amigorena, S., Raposo, G., Angevin, E., and Zitvogel, L. Malignant effusions and immunogenic tumour-derived exosomes. Lancet, *360:* 295–305, 2002.
12. Andre, F., Andersen, M., Wolfers, J., Lozier, A., Raposo, G., Serra, V., Ruegg, C., Flament, C., Angevin, E., Amigorena, S., and Zitvogel, L. Exosomes in cancer immunotherapy: preclinical data. Adv. Exp. Med. Biol., *495:* 349–354, 2001.
13. Amigorena, S. Cancer immunotherapy using dendritic cell-derived exosomes. Medicina (B. Aires), *60* (Suppl. 2)*:* 51–54, 2000.
14. Dolo, V., Ginestra, A., Cassara, D., Violini, S., Lucania, G., Torrisi, M. R., Nagase, H., Canevari, S., Pavan, A., and Vittorelli, M. L. Selective localization of matrix metalloproteinase 9, β1 integrins, and human lymphocyte antigen class I molecules

on membrane vesicles shed by 8701-BC breast carcinoma cells. Cancer Res., *58:* 4468–4474, 1998.
15. Ginestra, A., La Placa, M. D., Saladino, F., Cassara, D., Nagase, H., and Vittorelli, M. L. The amount and proteolytic content of vesicles shed by human cancer cell lines correlates with their *in vitro* invasiveness. Anticancer Res., *18:* 3433–3437, 1998.
16. Angelucci, A., D'Ascenzo, S., Festuccia, C., Gravina, G. L., Bologna, M., Dolo, V., and Pavan, A. Vesicle-associated urokinase plasminogen activator promotes invasion in prostate cancer cell lines. Clin. Exp. Metastasis, *18:* 163–170, 2000.
17. Rosania, G. R., Lee, J. W., Ding, L., Yoon, H. S., and Chang, Y. T. Combinatorial approach to organelle-targeted fluorescent library based on the styryl scaffold. J. Am. Chem. Soc., *125:* 1130–1131, 2003.
18. Staunton, J. E., Slonim, D. K., Coller, H. A., Tamayo, P., Angelo, M. J., Park, J., Scherf, U., Lee, J. K., Reinhold, W. O., Weinstein, J. N., Mesirov, J. P., Lander, E. S., and Golub, T. R. Chemosensitivity prediction by transcriptional profiling. Proc. Natl. Acad Sci. USA, *98:* 10787–10792, 2001.
19. Scherf, U., Ross, D. T., Waltham, M., Smith, L. H., Lee, J. K., Tanabe, L., Kohn, K. W., Reinhold, W. C., Myers, T. G., Andrews, D. T., Scudiero, D. A., Eisen, M. B., Sausville, E. A., Pommier, Y., Botstein, D., Brown, P. O., and Weinstein, J. N. A gene expression database for the molecular pharmacology of cancer. Nat. Genet., *24:* 236–244, 2000.
20. Simon, S. M., and Schindler, M. Cell biological mechanisms of multidrug resistance in tumors. Proc. Natl. Acad Sci. USA, *91:* 3497–3504, 1994.